Mechanics & Industry **24**, 37 (2023)
© A. Safa and S. Aissat, Published by EDP Sciences 2023
https://doi.org/10.1051/meca/2023035

Mechanics & Industry

Available online at:
www.mechanics-industry.org

REGULAR ARTICLE OPEN ACCESS

Analyzing the influence of lifter design and ball mill speed on grinding performance, particle behavior and contact forces

Ali Safa and Sahraoui Aissat*

Research Laboratory for Industrial Technologies, Department of Mechanical Engineering, Faculty of Applied Sciences, Ibn Khaldoun University, Tiaret, Algeria

Received: 12 May 2023 / Accepted: 12 September 2023

Abstract. Ball mills are the foremost equipment used for grinding in the mineral processing sector. Lifters are placed on the internal walls of the mill and are designed to lift the grinding media (balls) to a higher position. In the calculation of energy consumption in ball mills, classical theories mainly consider factors like the charge fill level, lifter dimensions, the number of lifters, and the rotational speed of the mill. This research recognizes the significance of lifter geometry and proposes a new lifter design aimed at optimizing the energy consumption and efficiency of ball mills. Simulation results by discrete elements obtained in this study were validated using experimental results. By conducting this comparative analysis, the aims of the study was to examine the impact of the new lifter's geometry and rotational speed of the mill on torque, power draw, particles behavior, and contact forces. The findings indicate that when the pitch of the lifters is increased, there is a reduction of 3.30% in torque and power consumption. Additionally, this change leads to an increase in the number of cataracting particles and a 6 to 7% increase in contact forces compared to lifters with a straight shape.

Keywords: Ball mill / helical lifter / grinding performance / particle behavior / contact forces / discrete element method (DEM)

1 Introduction

Ball mills are the most common type of fine grinding equipment. They are used in the chemical and pharmaceutical industries and the mineral processing industry for the production of cement [1].

These mills consume enormous amounts of electrical energy (50–60%); consequently, the cost of comminution accounts for roughly 60% of the overall investment in a beneficiation plant [2,3]. As a result, calculating power (or energy) is one of the essential factors in estimating operating costs and determining the best operating conditions for ball mills [4].

A variety of operating parameters, such as mill speed, the ball charge composition, charge filling, lifter type, and lifter number, all have a significant impact on ball milling grinding efficiency [3].

The grinding efficiency is a function of the quality of the final product, the energy (kWh) and the power (kW), which are used to determine the energy consumption of the mill [4].

EDEM stands for "Event-Driven Execution Model". It is a computational framework used for simulating the behavior of particulate materials such as powders, granules, and pellets in various industrial processes. The EDEM software uses the Discrete Element Method (DEM) to model the behavior of individual particles and how they interact with each other and with their surroundings.

This modelling method can be very beneficial for simulating and understanding the motion of the grinding media of different shapes and sizes in 3D mills [5], where it is difficult to gain insightful knowledge due to the complexity of the phenomena or the constraints of experimental investigation.

Moreover, DEM can show how lifter profiles affect mill power draw and media movement [6].

The number of publications that use the DEM method to study ball mills in depth has increased [7] and has attracted the interest of many researchers.

As lifters wear over their service life, this affects the motion of the grinding particles and the efficiency [8]. Therefore, lifters are changed when their maintenance cost becomes intolerable or when they reach a critical thickness and become susceptible to breaking with continued use [8]. The premature wear of the liners and lifters has a significant impact on the annual expenditure of grinding plants [5].

* e-mail: sahraoui.aissat@univ-tiaret.dz

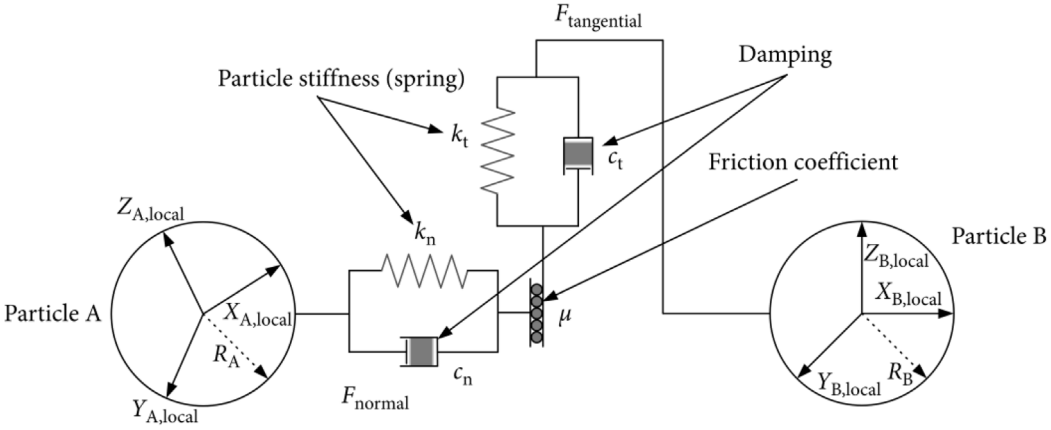

Fig. 1. Representation contact model between two particles (Hertz-Mindlin model) [16].

Several studies have been conducted recently for various types of lifters to examine the forces acting on the lifter bars, the wear of the lifter, the movement of the charge, the torque and the energy consumption of a ball mill. Here are some examples of what has been done:

Using a DEM simulator, Millsoft, Hlungwani et al. [6] investigated the impact of square and trapezoidal lifters on mill power draw and particle flow at various rotational speeds.

Djordjevic [9] examined the influence of lifter quality on the power draw of a tumbling mill using the PFC3D code. He concludes that this parameter has a considerable impact and shouldn't be ignored.

Makokha et al. [10–12] examine how the usage of cone-lifters affects milling capacity and productivity. Three liner profiles were tested, and an associated numerical simulation was utilized in their studies.

A new model of lifter bar wear is proposed by Rezaeizadeh et al. [13] to forecast the life and the evolution of these profiles, to reliably design lifters for a required life and provide a profile that offers optimal overall mill performance over the life of the lifters [13].

Using EDEM software, Powell et al. [5] predicted the lift bars' wear rate and developed a model to update worn lifter profiles gradually.

Bian et al. [14] studied the impact of lifter geometry, lifter number, and mill rotational speed on mill performance. In their work, the DEM simulations are compared with the experimental results.

Li et al. [15] simulate the particle motion in a ball mill for five distinct lifter shapes at various rotational speeds. Rectangular lifters and their impact on the ball mill's working efficiency have been given special consideration by them. Finally, they adopted the DEM-FEM method [15] to analyze the stress and deformation that lifters go through.

By conducting this study, researchers aim to gain a comprehensive understanding of the effects of new helical lift bar forms and mill speed on the torque, power consumption, particle behavior, and contact forces within the ball mill. The findings can then be used to optimize mill performance, enhance energy efficiency, reducing operational costs and assessing the wear and tear on the mill liners, grinding media, and other internal components.

2 Theory and methodology

2.1 Contact model

The Hertz-Mindlin model is the most commonly used in EDEM simulations [16] among the numerous contact models that have been used to model the contact between particles (Fig. 1).

The model in Figure 1 enables one to calculate forces that result from particle interaction in both normal and tangential directions [16]. Newton's second law can be applied to calculate acceleration.

By twice integrating the acceleration, the new particle locations are determined. Using the new positions for each particle, the new contact forces are calculated, and this cycle is repeated for each time step [16,17].

The normal force component is based on the Hertzian contact theory and the tangential force is based on the work of Mindlin and Deresiewicz [18].

The normal force (Fn) is given by equation (1) [19].

$$F_n = K_n\delta_n + C_n v_n \tag{1}$$

And the tangential force (F_t) is given by equation (2) [19].

$$F_t = min\left\{\mu F_n, K_t\int v_t dt + C_t v_t\right\} \tag{2}$$

The normal and tangential forces have damping components. The value of the normal damping coefficient is estimated from the coefficient of restitution [18,20], since the latter is a measure of the energy loss upon collision (Eq. (3)) [19].

$$C_n = -2\ln e\frac{\sqrt{k_n m^*}}{\sqrt{(\ln e)^2 + \pi^2}} \tag{3}$$

The equivalent mass m^* is given by equation (4) [19].

$$m^* = \left(\frac{1}{m_1} + \frac{1}{m_2}\right)^{-1} \tag{4}$$

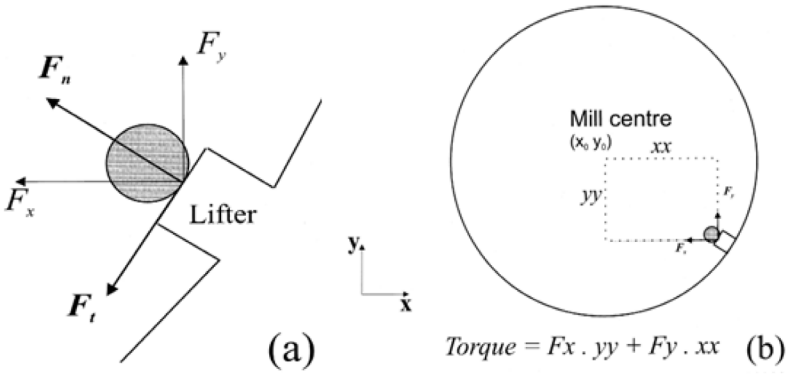

Fig. 2. (a) Contact between particle and lifter, (b) DEM torque calculation with Fx and Fy [19].

Table 1. Material properties and interaction parameters.

Material properties		Interaction parameters	
Poisson's ratio	0.25	Coefficient of restitution	0.5
Shear modulus (Pa)	7×10^{10} Pa	Coefficient of static friction	0.5
Density (kg/m^3)	7800	Coefficient of rolling friction	0.01

The particle is subject to a force equal to the sum of normal and tangential contact forces [19]. As indicated in Figure 2, this force is then decomposed into the x and y directions (Fx and Fy, respectively).

The DEM code EDEM is used to calculate the torque arm, and the torque is integrated into all contacts and all time steps [19].

The power drawn by the ball mill P (in Watt) is calculated using equation (5) [19]:

$$P = \frac{2\pi NT}{60} \tag{5}$$

With N mill speed in revolutions per minute and T torque (Nm).

2.2 Simulation time

The period between each iteration, or time step [21], must be extremely small ($< 10^{-6}$ s); it depends on the properties of the material (shear modulus), number of particles, the shape of the particles and particle size.

Equation (6) [17,21–24] was used to calculate the time step based on the Rayleigh time step. In our simulation, the time step is set to 20% of the Rayleigh time.

$$dt = T_{step} < \Delta_{critical} = T_{Rayleigh} = \frac{\pi R\sqrt{\frac{\rho}{G}}}{0,1631\nu + 0,8766} \tag{6}$$

With R the particle's radius, ρ its density, G the shear modulus, and ν the Poisson's ratio [21]. These parameters are given in Table 1.

2.3 Lifter profiles

In our DEM simulations, four lifter profiles (straight and helical with 2, 3, and 4 m pitch) were employed (Fig. 3). Their impacts on torque, power draw, particle motion, and contact forces were investigated.

Figure 4 depicts the mill's diameter and the dimensions of the trapezoidal lifting bars for the four considered profiles.

2.4 Mill characteristics

The parameters used in this article were selected regarding the work of Bian et al. The rotational speed varies between 60% and 100% of the critical speed calculated using equation (7) [25]. Other simulation parameters are listed in Table 2.

$$N = \frac{42.3}{\sqrt{D_i}}(rpm) \tag{7}$$

3 Results and discussion

3.1 Impact of rotational speed and lifter shape on torque and power draw

Figures 5 and 6 compare our simulated results using the EDEM software for various rotation speeds and lifter shapes with the experimental data of torque and mill power reported in Bian et al. work. The ball mill fill level is 35%, the lifter height is LH = 10 mm (Fig. 4), and the lifter bar number is 24.

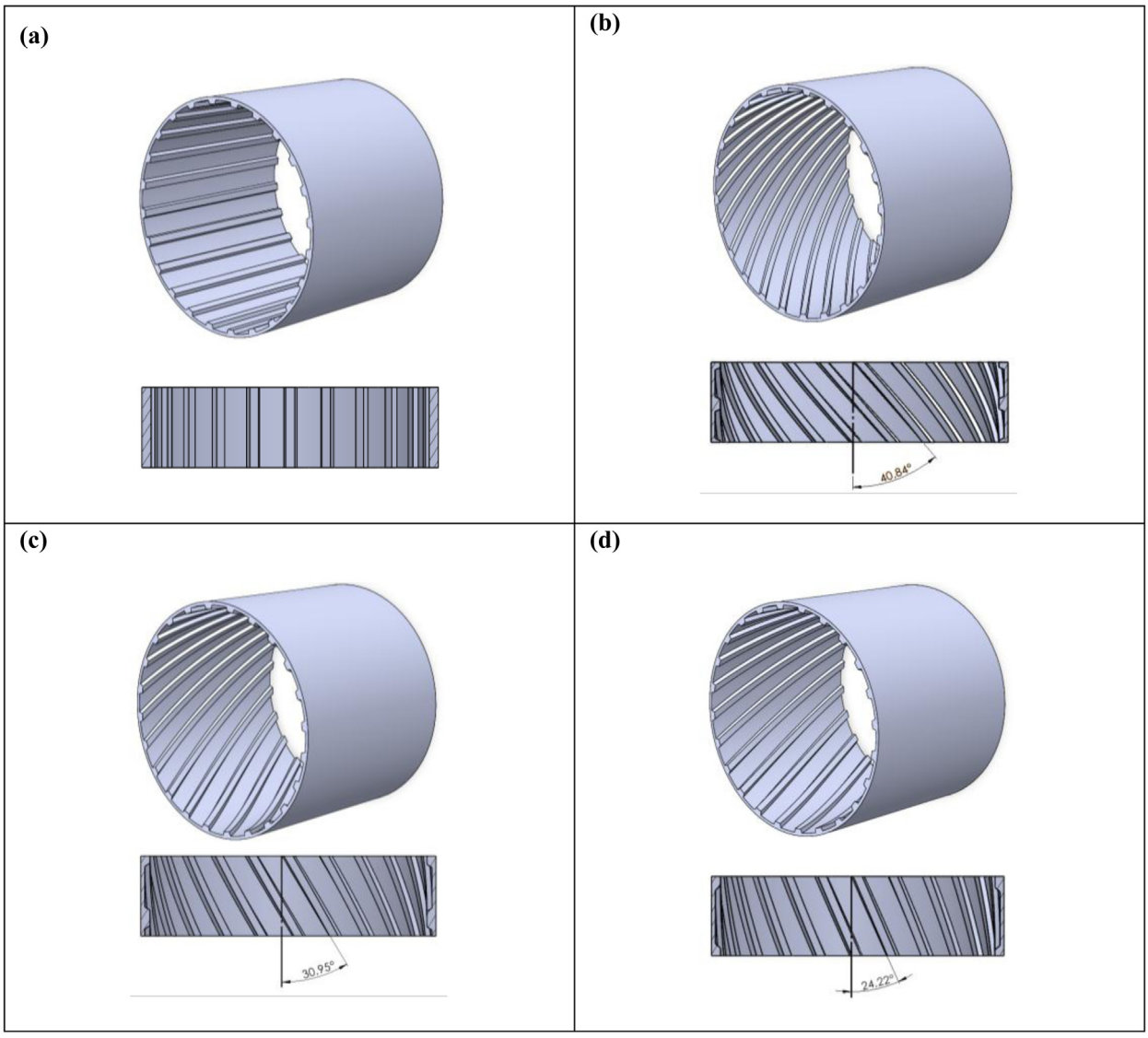

Fig. 3. 3D geometries of ball mills with (a) straight lifter; (b) helical pitch 2000 (HP2) lifter; (c) Helical pitch 3000 (HP3) lifter; (d) Helical pitch 4000 (HP4) lifter.

When the rotational speed is altered, DEM simulation and experimental curves are quite close (Fig. 5).

Maximum torque is achieved at a rotational speed between 70% and 80% for straight, HP3, and HP4 lifters. It reaches its maximum at a rotation rate between 70% and 75% for experimental results.

The torque decreases slightly until the speed reaches 90%. After this speed, the torque decreases by 6% to 14% compared to the experimental results. For HP2, the torque reaches its maximum at a rotation rate of 90%.

The power draw curves are remarkably similar. The values obtained by simulation fit the experimental ones well with a deviation of 2 to 9% between these values.

Figure 6 shows that the power draw curves show a continuous increase that is proportionate to the rotation rate. In our investigation, the mill power consumption reaches its maximum when $\omega = 100\%$.

The experimental curves of the power slightly declined when the rotational speed exceeded 90%, and the difference between the experimental curve and the other curves grew.

The power consumed by the mill shows lower values for the new helical lifters. This represents a significant advantage in terms of lowering the total cost of energy consumed by mills.

3.1.1 Comparison between the torque and the power values

Figure 7 shows the comparison of torque (Nm) and power (Watts) between our DEM simulation and the experimental results obtained in the work of Bian et al. for $\omega = 75\%$. It is observed that the helical lifter HP2 demonstrates the lowest values of torque and power.

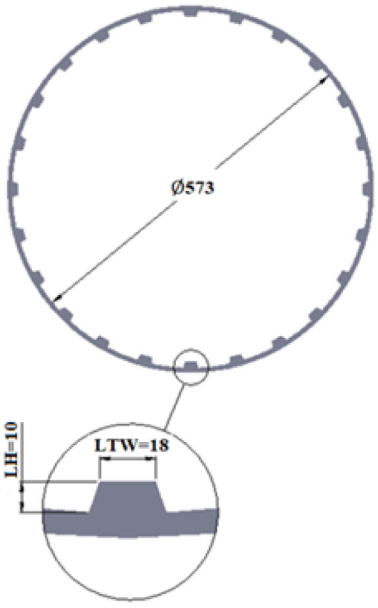

Fig. 4. Mill's diameter and the dimensions of the lifter used in the DEM simulation (LH: lifter height (mm); LTW: lifter top width (mm)).

Table 2. Ball mill dimensions and load.

	Parameters	Values
Ball mill	Internal diameter, mm	573
	Length, mm	160
Lifter	Number of lifters	24
	Dimensions of lifters, mm	10 × 18
Mill speed	Mill speed, rpm	55.87
	Rotational speed, rpm	(60%, 70%, 75%, 80%, 90%, 100%) × N 35
Grinding	Mill filling, %	

3.2 Impact of rotational speed and lifter shape on particles behavior

The effect of lifter design on particle behavior at different rotation rates ($\omega = 60$ to 100%) is examined in Figures 8, 9, and 10. The following simulation parameters were used: lifter number = 24, lifter height LH = 10 mm (Fig. 4), and fill level = 35%.

3.2.1 For HP2 lifters

In general, the particles follow cascading motion; they flow down the free surface of the charge. This zone is called the abrasion zone, colored in green, and is characterized by a low speed of particles.

The particles experience cataracting motion; they are propelled away from the surface in a distinctive parabolic trajectory. This region is often referred to as the impact zone and is characterized by a high speed of particles, which are colored in red. The blue color represents the dead zone where the particle velocity is zero.

The number of high-speed particles and the number of cataracting particles both significantly rise with increasing mill speed for all helical lifters.

For HP2, Figures 8a, 8b, 8c, and 8d show that most particles flow cascade, while a few flows cataract (Figs. 8e, 8f). The particles maximum velocity ranges from 1.89 m/s when the value of $\omega = 60\%$ to 3.52 m/s when the value $\omega = 100\%$. This increase is more visible between $\omega = 90\%$ and $\omega = 100\%$ (Fig. 11).

3.2.2 For HP3 lifters

The effect of HP3 lifters on particle behaviour for different rotation rates is illustrated in Figure 9.

3.2.3 For HP4 lifters

Considering the HP3 and HP4 lifters, there is a notable increase in the accumulation of cataracting particles as $\omega = 75\%$ (Figs. 9c, 9d, 9e, 9f, 10c, 10d, 10e, and 10f). These particles effectively spread across the entire surface area of the mill. Beyond $\omega = 75\%$, the maximum speed at which

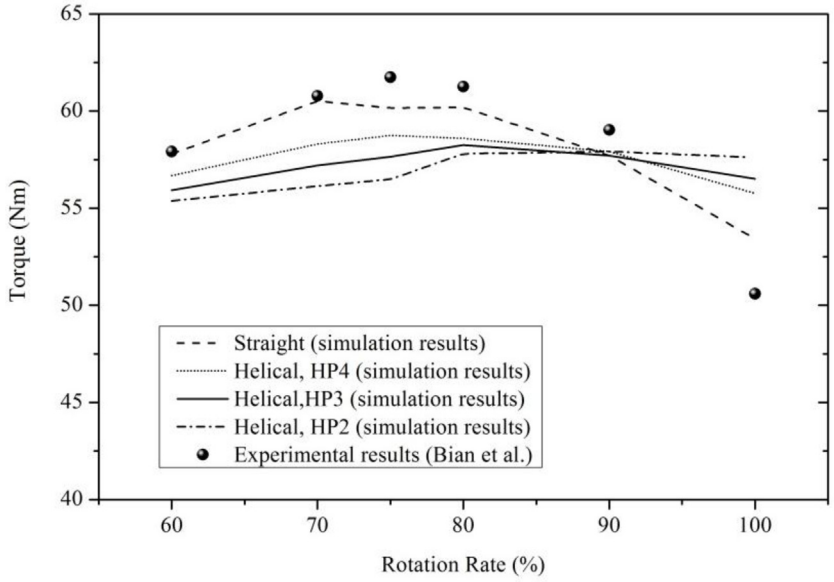

Fig. 5. Lifter geometry and rotational speed effects on mill torque.

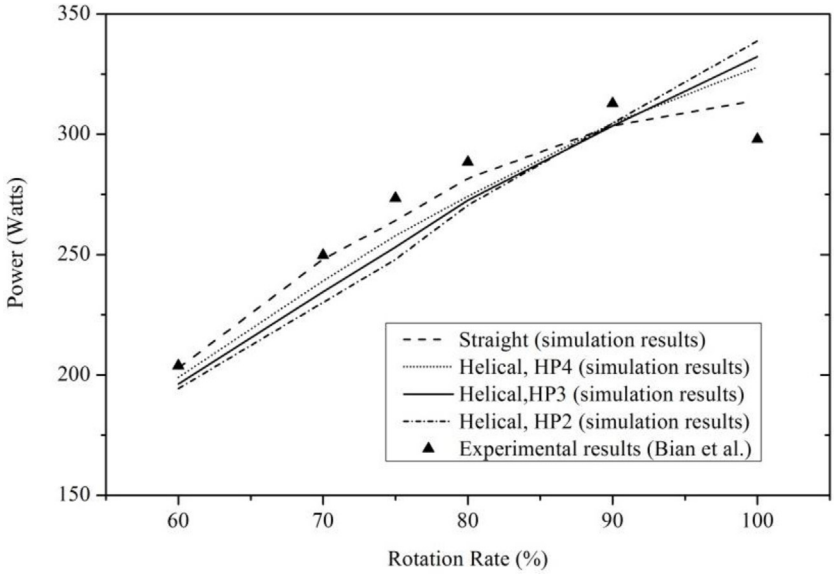

Fig. 6. Lifter geometry and rotational speed effects on power draw.

these particles are projected remains constant, on average around 3 m/s (Fig. 11). With a value of 3.41 m/s for the HP3 lifter and for $\omega = 90\%$.

At $\omega = 100\%$, the proportion of projected particles intensifies further and occupies practically the entire mill surface (Figs. 9f and 10f).

Increased lifter pitch has a considerable impact on particle behavior and breaking ability, as shown by Figures 8, 9, and 10.

3.2.4 Comparison of particles behavior

Figure 12 shows the comparison of particle behavior between our DEM simulation (Figs. 12b, 12c, 12d, and 12e) and the experimental results obtained in the work of Bian et al. (Fig. 12a). The used parameters are filling level = 35%, lifter height LH = 10 mm (Fig. 4), $\omega = 75\%$, and lifter number = 24.

According to Bian's [14] experimental results (Fig. 12a), flowing particles behave similarly as in the case of the right lifter (Fig. 12b), with a speed of 3.06 m/s.

When using a low-pitch lifter (HP2), the amount of cataracting particles and the percentage of high-speed particles both decrease (Fig. 12c). The particle velocity drops to 2.73 m/s.

The proportion of high-speed particles and the number of cataracting particles in the toe position both increase for HP3 (Fig. 12d) and HP4 (Fig. 12e). Their shoulder position is higher than the HP2 one. The speed of the particles is between 3.06 and 3.11 m/s.

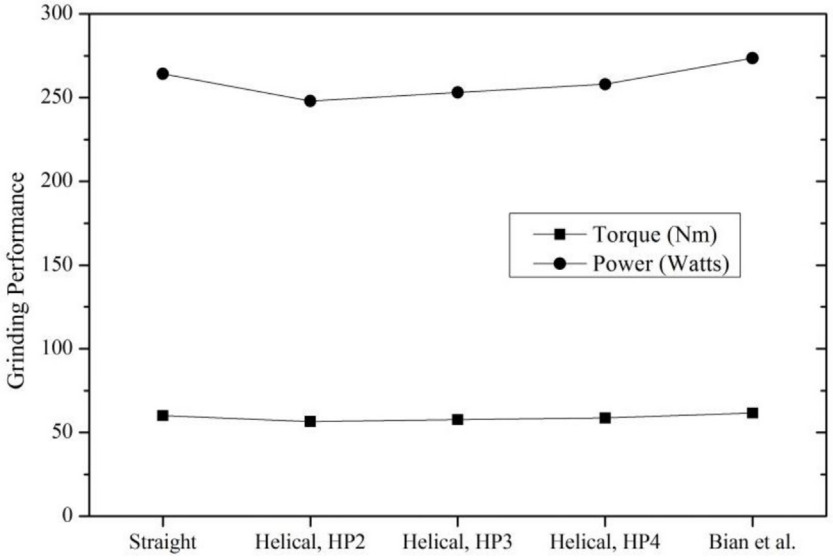

Fig. 7. Comparison between torque (Nm) and power (Watts) for $\omega = 75\%$.

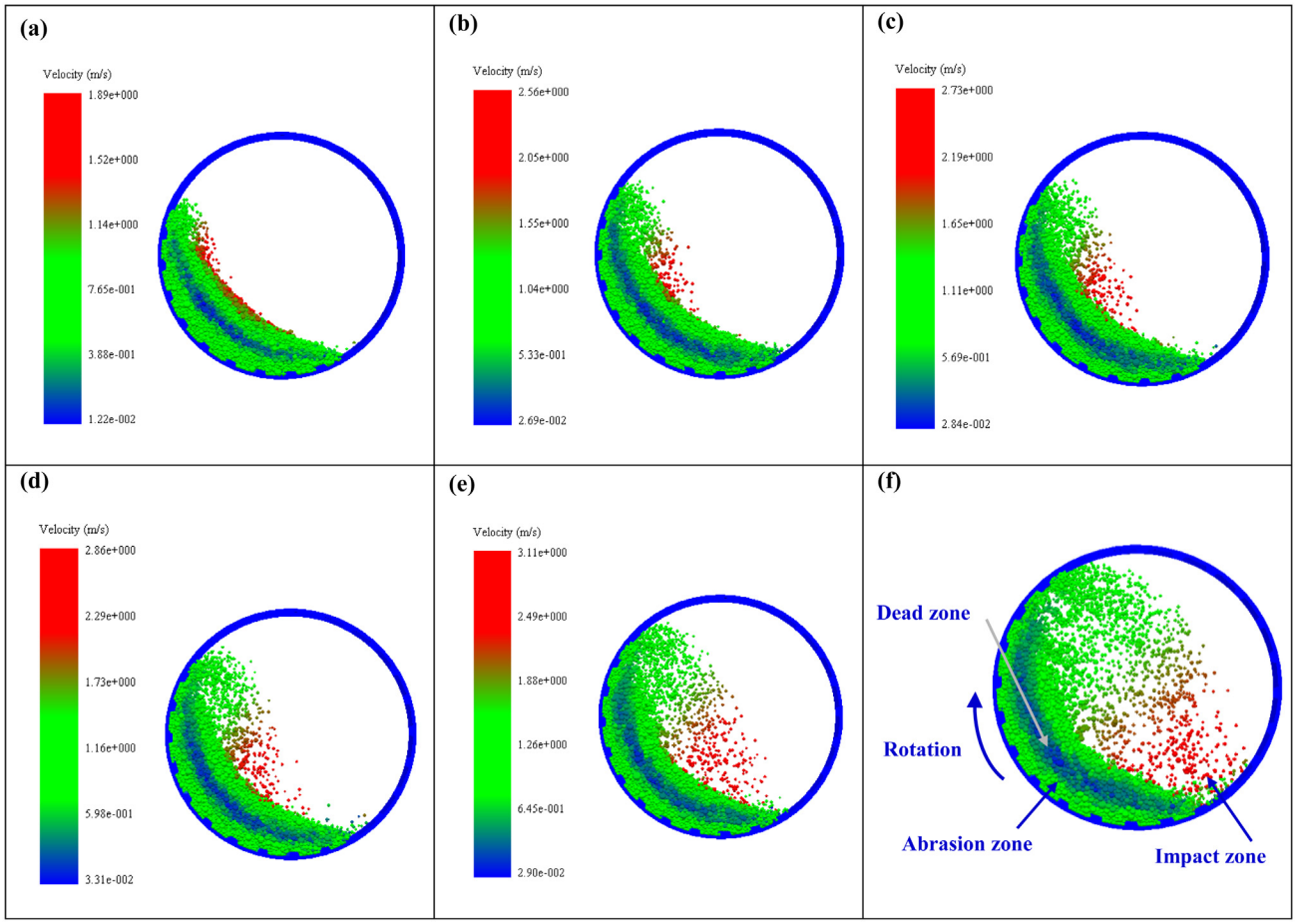

Fig. 8. Effect of HP2 lifters on particle behavior for different rotation rates: (a) $\omega = 60\%$; (b) $\omega = 70\%$; (c) $\omega = 75\%$; (d) $\omega = 80\%$; (e) $\omega = 90\%$; (f) $\omega = 100\%$.

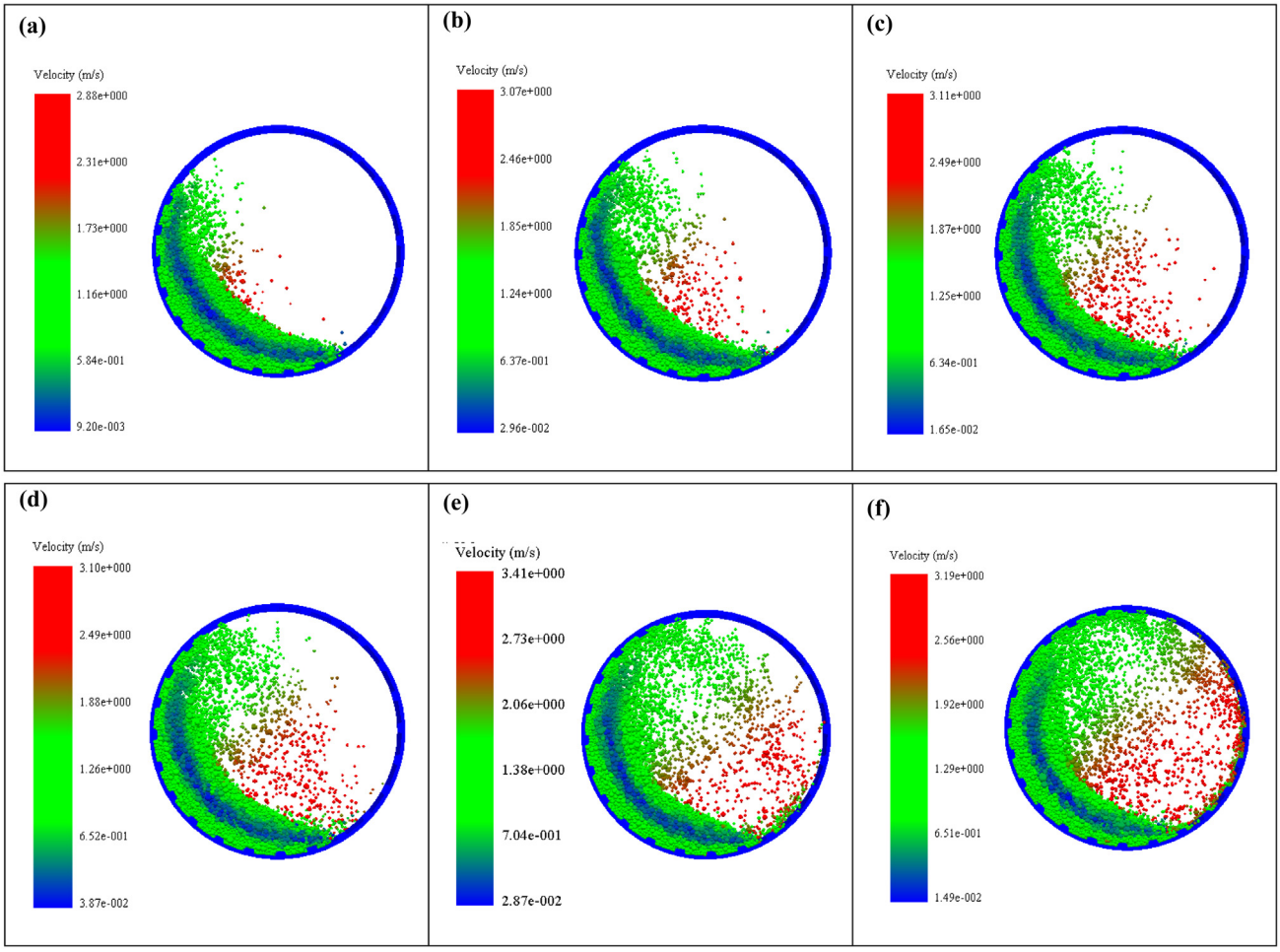

Fig. 9. Effect of HP3 lifters on particle behavior for different rotation rates: (a) $\omega = 60\%$; (b) $\omega = 70\%$; (c) $\omega = 75\%$; (d) $\omega = 80\%$; (e) $\omega = 90\%$; (f) $\omega = 100\%$.

3.3 Variation of the contact force with the shape of the lifter and rotational speed

3.3.1 Normal force of contact F_n

Figure 13 shows the normal forces F_n at rotational speeds $\omega = 60$ to 100% and for different lifter geometries.

3.3.2 Tangential contact force F_t

The mill speed has significant effect on tangential force. Figure 14 rates the changes in the tangential contact force F_t for rotational speeds between 60 and 100% and for various lifter geometries.

The contact forces (F_n and F_t) are at their highest for $\omega = 80\%$ for the straight lifter and for $\omega = 90\%$ for HP3 and HP4. Once these velocities are surpassed, the contact forces start to decrease. This decrease is caused by the centrifugal motion of particles that adhere to the drum's wall, resulting in a reduction of the impact energy.

The HP2 lifters demonstrates elevated levels of these forces, with their intensities progressively growing as the rotational speed rises, providing advantages for the grinding process. This is due to the larger contact surface of the helical lifters which is maintained at all times, distributing the load more evenly. This enables them to withstand higher contact loads.

3.3.3 Comparison of contact forces values

According to Figure 15 (established for $\omega = 75\%$), it becomes evident that the normal contact force plays a more crucial role in material grinding and has a greater impact on the overall grinding efficiency compared to the tangential force.

The ratio of the tangential forces to the normal forces is 0.35 at $\omega = 75\%$.

4 Conclusions

In this work a new lifter design is proposed. The aim was to compare the torque, power consumption, particle behavior, and contact forces of a ball mill with the experimental results obtained in the work of Bian et al. The results obtained in this study allow drawing the following conclusions:

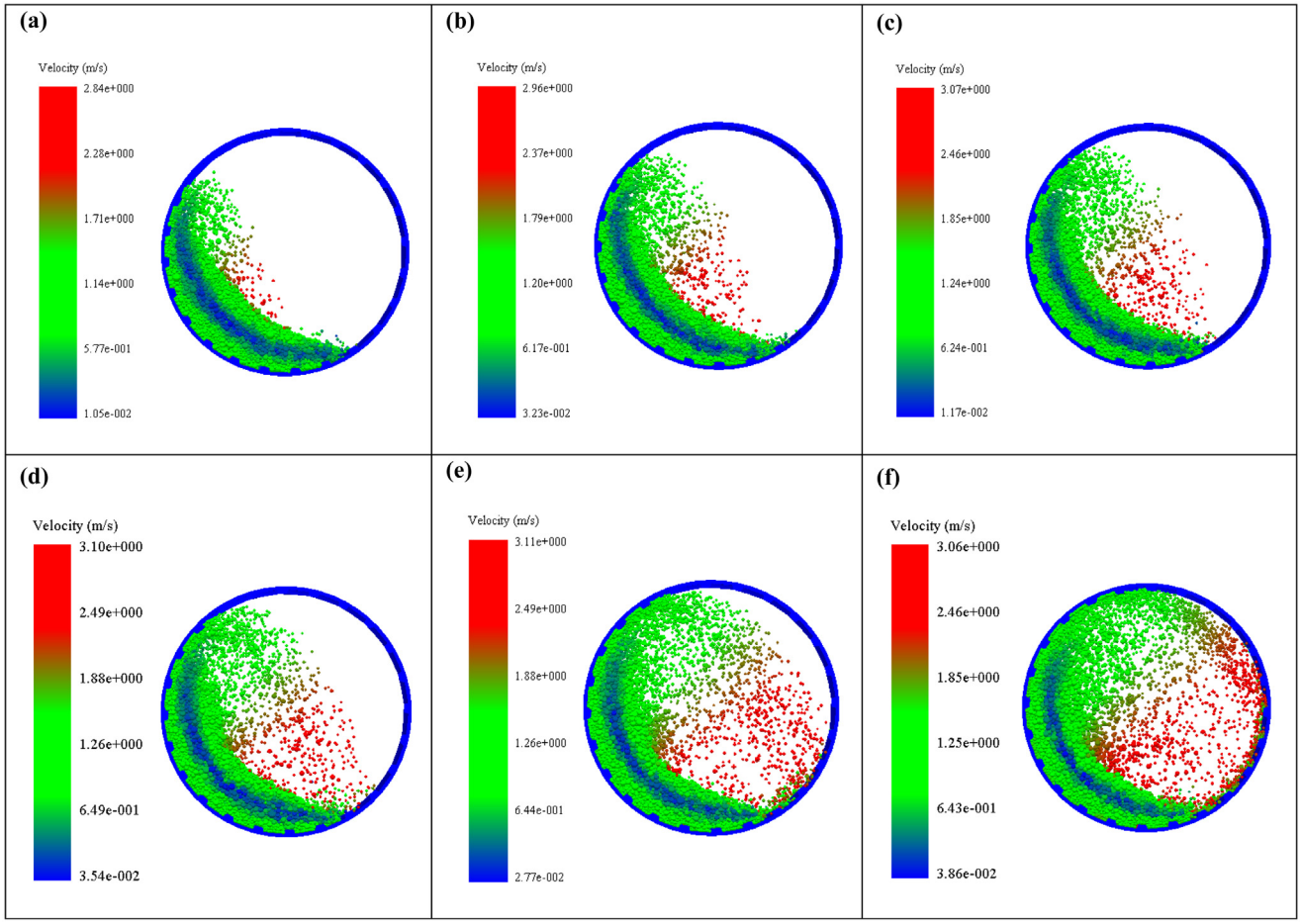

Fig. 10. Impact of HP4 lifters on particle behavior for various rotation rates: (a) $\omega = 60\%$; (b) $\omega = 70\%$; (c) $\omega = 75\%$; (d) $\omega = 80\%$; (e) $\omega = 90\%$; (f) $\omega = 100\%$.

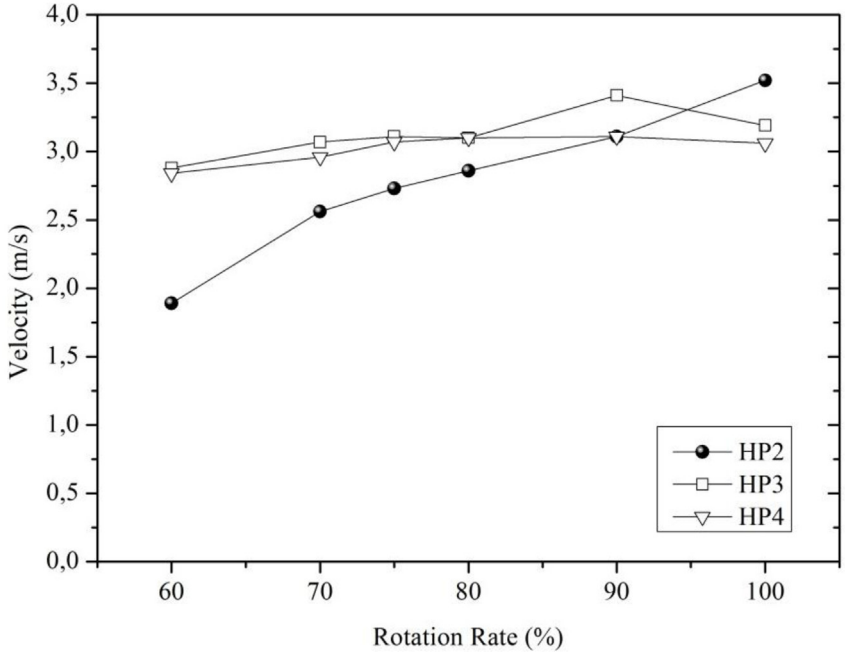

Fig. 11. Comparing the velocities of helical lifters' particles.

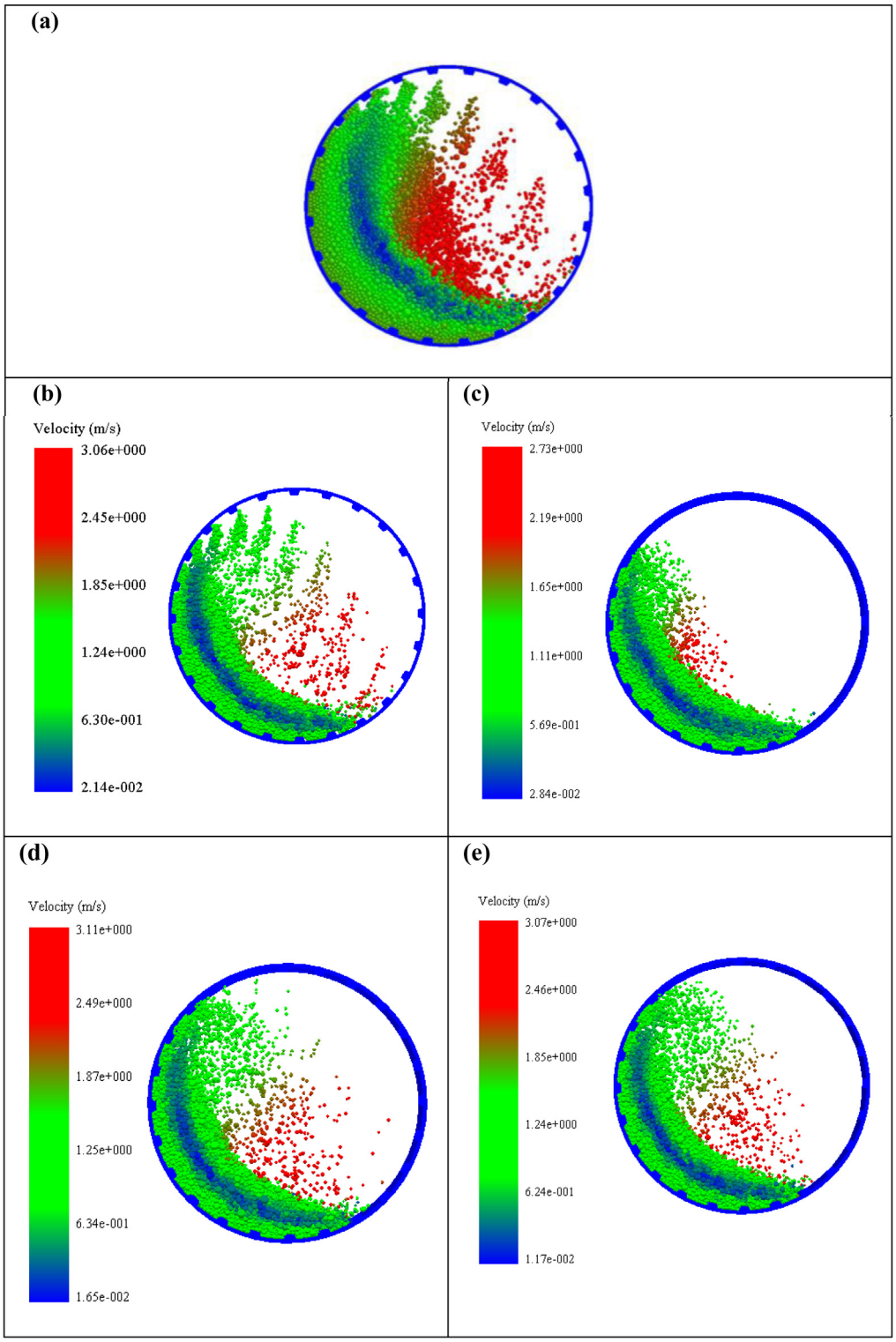

Fig. 12. Particles speed diagram ($\omega = 75\%$) for (a) experiment result, Bian et al.; (b) straight lifter; (c) HP2 lifter; (d) HP3 lifter; (e) HP4 lifter.

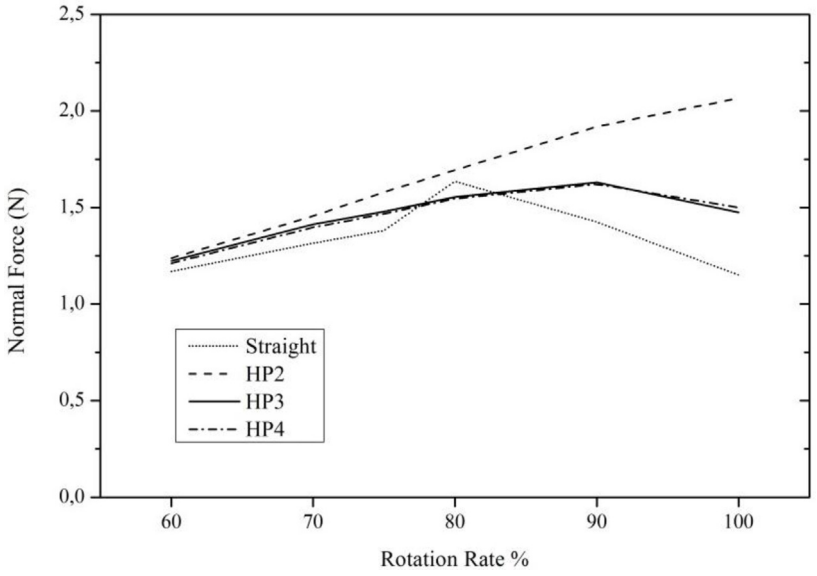

Fig. 13. Influence of lifter shape and rotational speed on the variation of normal contact force F_n.

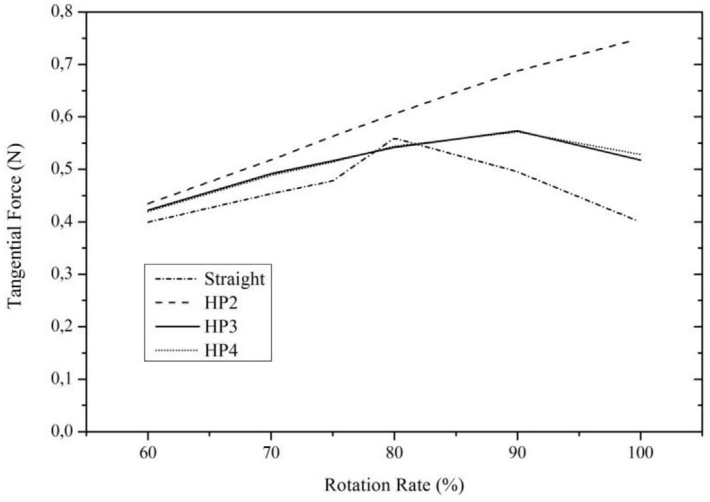

Fig. 14. Influence of lifter shape and rotational speed on the variation of tangential contact force F_t.

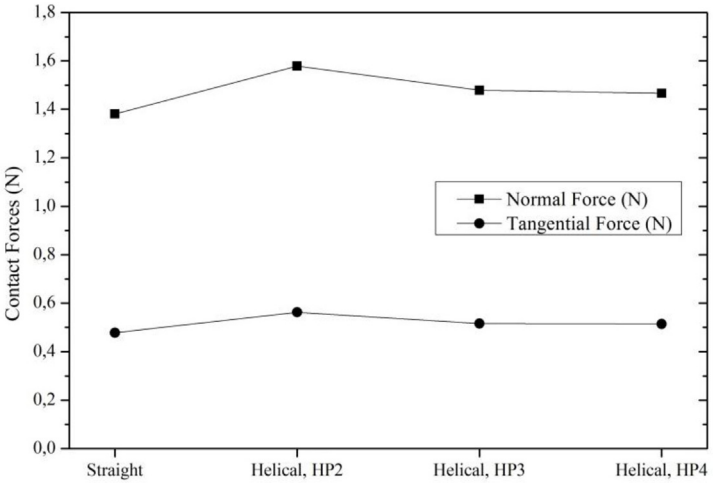

Fig. 15. Comparison between the normal force and the tangential force at $\omega = 75\%$.

- The objective of this study has been successfully accomplished by conducting a qualitative validation of the simulation findings, comparing them to the experimental outcomes conducted by Bian et al. These findings exhibit consistency and agreement.
- The mill torque increases and peaks between 70% and 75%, which is consistent with the experimental results of Bian et al. It declines after this speed. The simulated results for the helical lifters are lower compared to the experimental data, showing a Mean Absolute Error (MAE) is 2 to 4 Nm.
- When the speed of rotation rises, the helical elevators exhibit lower power consumption values. The Mean Absolute Error (MAE) is 14 to 20 Watts between the experimental data and the measured values.
- As the pitch of the helical lifter increases from HP2 to HP3 and HP4, there is a noticeable increase in the abundance of high-speed particles, which creates a cataracting medium. This movement has a considerable influence on both the effectiveness of the grinding process and the quality of the end product.
- The particle speed in HP2 nearly doubles when transitioning from $\omega = 60\%$ to 100%. However, in the case of HP3 and HP4, the speed gradually rises from $\omega = 60\%$ to 75% and then remains constant beyond $\omega = 75\%$.
- The normal force holds greater significance in material grinding and exerts a more substantial influence on the overall efficiency of the grinding process in comparison to the tangential force.
- By employing helical-shaped lifters as suggested in this study, we have achieved a reduction in power consumption of the mill, an increase in the required contact forces for the grinding process, and a better understanding of particle behavior. However, it is necessary to validate these findings by conducting laboratory experiments for further comparison.

Nomencluture

K	Particle stiffness (N/m)
C	Dash-pot damping coefficient
v	Relative velocity of the particles (m/s)
dt	Time step of the simulation (s)
e	Coefficient of restitution
m^*	Effective (equivalent) mass (kg)
δ	Particle overlap (mm)
μ	Coefficient of friction

Authors' contributions

Methodology, Ali Safa and Sahraoui Aissat; EDEM software, Ali Safa; Analysis and investigation, Ali Safa and Sahraoui Aissat; bibliographical sources, Ali Safa; writing original and review the manuscript, Ali Safa and Sahraoui Aissat. The final published version of the paper has been read and approved by all authors.

Funding

This research work received no external funding from natural or legal persons.

Data availability statement

The data that support the findings of this study are available on request from the corresponding author.

Conflicts of interest

The authors declare that there is no conflict of interest.

References

[1] I. de Camargoa, J. Fiore, P. Lovoa, R. Erberelia, C.A. Fortulana, Influence of media geometry on wet grinding of a planetary ball mill, Mater. Res. **22**, 1–6 (2019)
[2] S. Liang, Y. Cao, G. Fan, The effect of grinding media on mineral breakage properties of magnetite ores, Geofluids, 1–9 (2021). doi.org/10.1155/2021/1575886
[3] G.S. Abdelhaffez, A.A. Ahmed, H.M. Ahmed, Effect of grinding media on the milling efficiency of a ball mill, Mining-Geology-Petroleum Eng. Bull. 171–177 (2021). DOI: 10.17794/rgn.2022.2.14
[4] S. Chehreghani, H.H. Gharehgheshlagh, S. Haghikia, Power consumption management and simulation of optimized operational conditions of ball mills using the morrell power model: a case study, Mining-Geology-Petroleum Eng. Bull. 123–135 (2021). DOI: 10.17794/rgn.2022.2.11
[5] M.S. Powell, N.S. Weerasekara, S. Cole, R.D. LaRoche, J. Favier, DEM modelling of liner evolution and its influence on grinding rate in ball mills, Miner. Eng. **24**, 341–351 (2011)
[6] O. Hlungwani, J. Rikhotso, H. Dong, M.H. Moys, Further validation of DEM modeling of milling: effects of liner profile and mill speed, Miner. Eng. **16**, 993–998 (2003)
[7] D. Daraio, J. Villoria, A. Ingram, A. Alexiadis, E. Hugh Stitt, M. Marigo, Validation of a discrete element method (DEM) model of the grinding media dynamics within an attritor mill using positron emission particle tracking (PEPT) measurements, Appl. Sci. **9**, 4816 (2019)
[8] J. Tshibangu Kalala, Discrete Element Method Modeling of Forces and Wear on Mill Lifters in Dry Ball Milling, Ph.D. Thesis, University of Witwatersrand, Johannesburg, 2008
[9] N. Djordjevic, Discrete element modelling of the influence of lifters on power draw of tumbling mills, Miner. Eng. **16**, 331–336 (2003)
[10] A.B. Makokha, M.H. Moys, Towards optimizing ball-milling capacity: effect of lifter design, Miner. Eng. **19**, 1439–1445 (2006)
[11] A.B. Makokha, M.H. Moys, Effect of cone lifters on the discharge capacity of the mill product: case study of a dry laboratory-scale air-swept ball mill, Miner. Eng. **20**, 124–131 (2007)
[12] A.B. Makokha, M.H. Moys, M.M. Bwalya, K. Kimera, A new approach to optimizing the life and performance of worn liners in ball mills: experimental study and DEM simulation, Int. J. Miner. Process **84**, 221–227 (2007)

[13] M. Rezaeizadeh, M. Fooladi, M.S. Powell, S.H. Mansouri, N.S. Weerasekara, A new predictive model of lifter bar wear in mills, Miner. Eng. **23**, 1174–1181 (2010)
[14] X. Bian, G. Wang, H. Wang, S. Wang, W. Lu, Effect of lifters and mill speed on particle behavior, torque, and power consumption of a tumbling ball mill: experimental study and DEM simulation, Miner. Eng. **105**, 22–35 (2017)
[15] Z. Li, Y. Wang, W. Lin, K. Li, Studies on the performance of ball mill with liner structure based on DEM, J. Eng. Technol. Sci., **50**, 157–178 (2018)
[16] P. Muhayimana, JK Kimotho, M.K. Ndeto, H.M. Ndiritu, Effects of lifter configuration on power consumption of small scale ball mill, J. Sustain. Res. Eng. **4**, 171–183 (2018)
[17] S. Kolahi, M.J. Chegeni, K.S. Shabani, Investigation of the effect of industrial ball mill liner type on their comminution mechanism using DEM, Int. J. Min. Geo-Eng. **55**, 97–107 (2021)
[18] T. Yasunaga, M. Yoshida, A. Shimosaka, Y. Shirakawa, T. Andoh, H. Ichikawa, N. Ogawa, H. Yamamoto, Mathematical modelling of coating time in dry particulate coating using mild vibration field with bead media described by DEM simulation, Adv. Powder Technol. **33**, 103779 (2022)
[19] M.A. van Nierop, G. Glover, A.L. Hinde, M.H. Moys, A discrete element method investigation of the charge motion and power draw of an experimental two-dimensional mill, Int. J. Miner. Process. **61**, 77–92 (2001)
[20] P.K. Cleary, P. Owen, Effect of particle shape on structure of the charge and nature of energy utilization in a SAG mill, Miner. Eng. **132**, 48–68 (2019)
[21] EDEM, User Guide; DEM Solut. (Ltd. 2017)
[22] M. Marigo, E.H. Stitt, Discrete element method (DEM) for industrial applications: Comments on calibration and validation for the modelling of cylindrical pellets, KONA Powder Part. J. **32**, 236–252 (2015)
[23] S. Rosenkranz, S. Breitung-Faes, A. Kwade, Experimental investigations and modelling of the ball motion in planetary ball mills, Powder Technol. **212**, 224–230 (2011)
[24] K. Kyong-Chol, J. Tao, K. Nam-Il, K. Cholu, Effects of ball-to-powder diameter ratio and powder particle shape on EDEM simulation in a planetary ball mill, J. Indian Chem. Soc. **99**, 100300 (2022)
[25] H. Usman, Measuring the efficiency of the tumbling mill as a function of lifter configurations and operating parameters, Ph.D. Thesis, Colorado School of Mines, 2015

Cite this article as: A. Safa and S. Aissat, Analyzing the influence of lifter design and ball mill speed on grinding performance, particle behavior and contact forces, Mechanics & Industry **24**, 37 (2023)